PHYSICAL REVIEW C **71**, 011301 (2005)

Lifetimes of excited states in octupole-collective ^{142,144}Ba nuclei

D. C. Biswas,[1,*] A. G. Smith,[1] R. M. Wall,[1] D. Patel,[1] G. S. Simpson,[1] D. M. Cullen,[1] J. L. Durell,[1] S. J. Freeman,[1] J. C. Lisle,[1] J. F. Smith,[1] B. J. Varley,[1] T. Yousef,[1] G. Barreau,[2] M. Petit,[2] C. Theisen,[3] E. Bouchez,[3] M. Houry,[3,†] R. Lucas,[3] B. Cahan,[3,‡] A. Le Coguie,[3] B. J. P. Gall,[4] O. Dorvaux,[4] and N. Schulz[4]

[1]*Department of Physics and Astronomy, University of Manchester, Manchester, M13 9PL, UK*

[2]*Centre d'Études Nucléaires de Bordeaux-Gradignan (CENBG), F-33175 Gradignan Cedex, France*

[3]*CEA/Saclay, F-91191 Gif-sur-Yvette Cedex, France*

[4]*Institut de Recherches Subatomiques, CNRS-IN2P3, Université Louis Pasteur, F-67037 Strasbourg, France*

(Received 16 February 2004; published 6 January 2005)

Lifetimes of excited states have been measured for the positive-parity rotational bands in neutron-rich ^{142,144}Ba as well as the 7^- and 9^- states of the negative-parity band in ^{144}Ba using the differential Doppler shift method. The deduced quadrupole moment, Q_t, of the positive-parity band decreases with angular momentum and overall shows good agreement with earlier measurements. The measured lifetimes of 7^- and 9^- states are used to determine the electric dipole moment, $D_0 = 0.17(3)$ and $0.09(1)$ e fm, respectively, in the negative-parity octupole band of ^{144}Ba.

DOI: 10.1103/PhysRevC.71.011301 PACS number(s): 21.10.Tg, 23.20.−g, 25.85.Ca, 27.60.+j

The shapes of excited nuclear states are strongly influenced by the rearrangement of the constituent nucleons and their collective motion. Various theoretical models have been put forward to describe the complex shape evolution of deformed nuclei, and the existence of pear-shaped octupole deformation was predicted from reflection-asymmetric mean field calculations [1–6]. These "quasi-molecular" states have shapes that are similar to the asymmetric molecules such as HCl, with rotational bands of alternating-parity states. The occurrence of an island of octupole deformation for $Z \sim 56$ and $N \sim 88$ and light actinides ($Z \sim 90$ and $N \sim 134$) has been verified from the observation of low-lying negative-parity states connected to yrast positive-parity states by strong electric dipole ($E1$) transitions [7–13]. The electric dipole moment, D_0, which arises from the displacements of the centers of proton and neutron distributions in the nucleus, is expected to be significantly large for the octupole-deformed nuclei. In the past, D_0 has been determined experimentally using the measured $B(E1)/B(E2)$ ratios and an estimated transition quadrupole moment (Q_t) [7–9]. However, the quadrupole moment does not remain constant with the angular momentum of the excited states [14] and hence the deduced D_0 values will depend on the model assumptions. Although nuclear shape correlations are studied in several neutron-rich nuclei, the influence of the octupole deformation on the lifetimes of the excited states has not been explored. The motivation of measuring the lifetimes of the excited states is to determine the quadrupole and electric dipole moments which provide crucial information on the octupole correlations in nuclei.

Lifetimes of low-lying states in some neutron-rich nuclei have been measured earlier using the Doppler profile method [15,16], the direct timing of β-delayed γ rays [17] and also the recoil distance method [18]. Recently, the differential Doppler shift method (DDSM) has been used for measuring lifetimes covering a range from picoseconds to nanoseconds for many neutron-rich nuclei produced in spontaneous fission [19–23]. In the present work, we report the measured lifetimes of 2^+ and 4^+ states in ^{142}Ba as well as the $2^+, 4^+, 6^+, 8^+, 7^-$, and 9^- states in ^{144}Ba. The lifetime measurements have been carried out using the differential-plunger technique, together with Euroball and the SAPhIR multidetector array. A ^{252}Cf source of total 60 μCi activity, was electroplated over a circular area of 5 mm in diameter at the center of the front face of a hollow Cu cylinder. The experiment was performed by mounting the plunger device and the SAPhIR array inside the Euroball detector array that comprised clover, cluster, and tapered Ge detectors. The special configuration of the SAPhIR array used in this experiment had 48 solar cells, each of area 12 mm^2, and was mounted at a distance of 8 cm from the center of the Euroball array. More detail of the experimental arrangement and the differential plunger device has been reported earlier [19].

For each fission event, one of the fragments emanating from the ^{252}Cf source stops in the Cu backing. The other fission fragment, when emitted at angles less than 50° to the Euroball axis, passes through a stretched Au/Ni foil (thickness ∼2–3 mg cm^{-2}) losing about 50% of its energy before being detected in the SAPhIR array. The source-to-foil distance (D) was varied by changing the position of the source, and measurements were carried out for 17 distance settings ranging from 14 to 7630 μm. The zero point of the distance scale was set through an examination of the capacitance as a function of distance. Distances relative to this point were taken directly from the micrometer readings. The uncertainty in the measurement of D is less than 10% for large distances (>200 μm) and is about 20% for small distances. The

*Permanent address: Bhabha Atomic Research Centre, Mumbai-400085, India.

†Present address: CEA/DIF DCRE/SDE/LDN, BP 12, F-91680 Bruyères-le-Châtel, France.

‡Present address: GANIL, Boulevard Henri Becquerel, BP 5025, F-14076 Caen, France.

γ-ray energy, time, and detector number were recorded onto magnetic tape when an event was detected by the Euroball and SAPhIR. After energy calibration of the solar cells and the γ-ray detectors, the data were sorted into two-dimensional γ-γ coincidence matrices with a condition set on the fragment energy to select only the heavy fragments entering the SAPhIR cells. This included the γ rays emitted from fragments of different velocities viz: (i) light fission fragments stopped in the Cu backing, (ii) heavy fission fragments moving with full velocity ($\beta_{\rm FS}$) before the foil, and (iii) heavy fission fragments moving with partial velocity ($\beta_{\rm PS}$) after the foil.

For data analysis, the level schemes of ^{142,144}Ba isotopes were taken from earlier measurements [7,9]. The Doppler corrections applied to the measured γ ray of energy E emitted at an angle θ to the direction of the fission fragment were as follows:

$$E_{\rm FS} = \frac{E}{(1 + \beta_{\rm FS}\cos\theta)} \quad (1)$$

and

$$E_{\rm PS} = \frac{E}{(1 + \beta_{\rm PS}\cos\theta)} \quad (2)$$

where $E_{\rm FS}$ and $E_{\rm PS}$ are known as the fully and partially shifted γ-ray energies, respectively. For each distance, the two-dimensional matrices were produced for $E_{\rm PS}$ vs, $E_{\rm PS}$, $E_{\rm PS}$ vs, $E_{\rm FS}$, and $E_{\rm FS}$ vs, $E_{\rm FS}$. These two-dimensional matrices were utilized to apply single gates to either partially or fully shifted decays from the nucleus of interest to view either $E_{\rm PS}$ or $E_{\rm FS}$. To ensure that the gates on the Doppler shifted energies were velocity sensitive, only detectors with angles for which $\cos\theta > 0.5$ are considered in the analysis. The solar cells suffered from a pulse-height degradation during the course of the experiment due to radiation damage, and a time-dependent calibration was applied for the velocity calculation. However, the deteriorating energy resolution of the solar cells did not have any significant effect on the velocity calculation and, hence, the Doppler correction could be applied satisfactorily.

Figure 1 shows typical energy spectra of $E_{\rm FS}$ for the distances of 14, 106, 630, and 7630 μm with gates on $2^+ \rightarrow 0^+$ (199.3 keV) and $6^+ \rightarrow 4^+$ (431.4 keV) in ^{144}Ba. The line shape of the γ-ray energy spectra shows a gradual change from the smaller distances to the larger distances. The fraction of γ rays emitted from the fragment before and after the foil, depends on the distance D and the lifetime of the excited states. The energy spectra for the fully shifted (indexed as FS) and partially shifted (indexed as PS) γ-ray energy of ^{144}Ba are plotted in Fig. 2, for the shortest ($D = 14$ μm) as well as largest distance ($D = 7630$ μm). The line shape spectra were obtained in two different ways: first setting a gate on $E_{\rm FS}$ and taking a projection on the $E_{\rm FS}$ of yrast transitions for ^{144}Ba to obtain the FS energy spectra. Second, the PS energy spectra were obtained from a gate on the partially shifted lines in $E_{\rm PS}$ and taking a projection on the $E_{\rm PS}$. To increase the statistics for the $E1$ transitions, the gates were set on the three dominant yrast transitions of the positive-parity band, and the data were added together. At the short distances, the γ rays for all the transitions are predominantly emitted after passing through the foil. A single peak is observed at the expected position in the PS plots, once the Doppler correction is applied [see Fig. 2(a)]. In the FS plots, the fully shifted component was represented by a Gaussian center on the known γ-ray energy, whereas the wrongly Doppler-corrected partially shifted components appear as broad bumps on either sides of $E_{\rm FS}$. At large distances, the γ-ray spectrum of the $2^+ \rightarrow 0^+$ transition (for which the lifetime is expected to be long) will be an admixture of fully and partially shifted components and appear as a broad peak both in PS as well as FS plots. However, for all other transitions, the γ rays are mostly emitted before the foil and the spectra will have wrongly corrected fully shifted components in the PS plots [see Fig. 2(b)]. The complementary behavior has been observed in the FS plots, where a single peak is seen at the expected energy.

The evolution of line shapes for different excited states is very sensitive to the source-to-foil distances. The data corresponding to the full range of distances were fitted together, with a common centroid, width parameters, and background regions. The fit to the PS and FS line shape spectra (following the procedure discussed in Ref. [19]) are obtained for all the transitions, and the fits are shown in Fig. 2 by the superimposed lines. The two-component fit of each

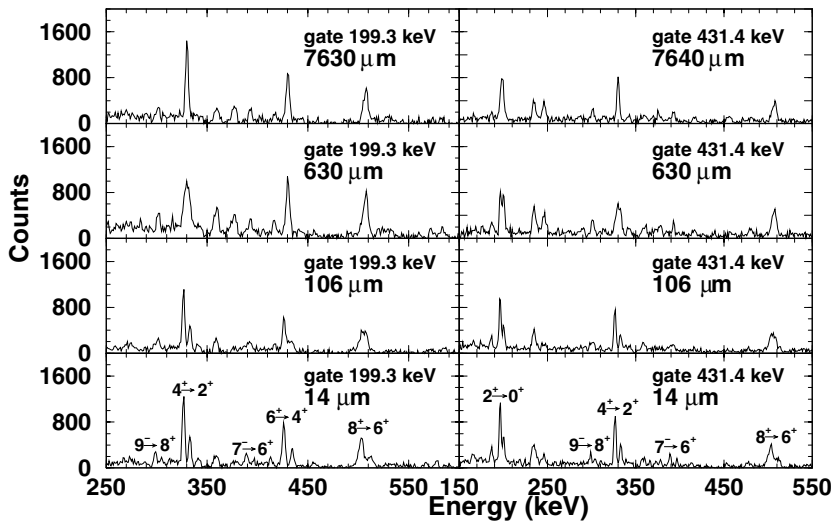

FIG. 1. Typical fully shifted γ-ray energy spectra for the distances of 14, 106, 630, and 7630 μm with gates on $2^+ \rightarrow 0^+$ (199.3 keV) and $6^+ \rightarrow 4^+$ (431.4 keV) transitions of ^{144}Ba.

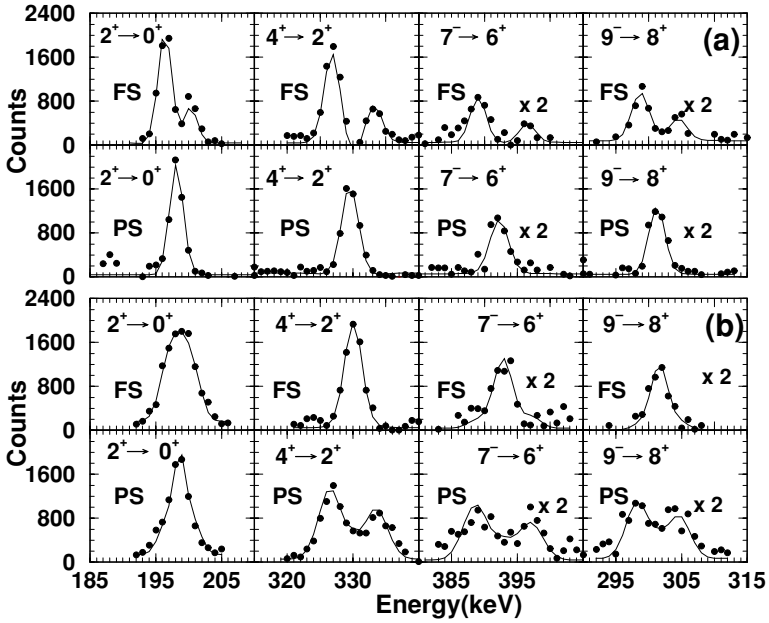

FIG. 2. The γ-ray energy spectra of ^{144}Ba for the $E2$ transitions $2^+ \rightarrow 0^+$ (199.3 keV) and $4^+ \rightarrow 2^+$ (330.7 keV); the $E1$ transitions: $7^- \rightarrow 6^+$ (393.8 keV) and $9^- \rightarrow 8^+$ (302.3 keV) projected on the partially shifted (indexed as PS) as well as fully shifted (indexed as FS) γ-ray energies for (a) $D = 14$ μm and (b) $D = 7630$ μm. The fits are shown with solid lines.

γ-ray line shape spectrum provides the fractional count of the partially shifted ($F_{\rm PS}$) component, which is obtained from the ratio of the partially shifted counts ($N_{\rm PS}$) to the total counts in partially and fully shifted ($N_{\rm FS}$) components, i.e., $F_{\rm PS} = N_{\rm PS}/(N_{\rm PS} + N_{\rm FS})$. From the fitting of the line shape spectra in the PS and FS plots, the average value of $F_{\rm PS}$ is obtained for each distance.

To obtain the mean lifetime (τ) of different excited states, $F_{\rm PS}$ is plotted as a function of distance D. These data are fitted by simulating the decays of the known level scheme in which the lifetimes of various states were free parameters in a fit to the $F_{\rm PS}$ data. The consistent fitting of the decay curves corresponds to a numerical solution of the coupled equations that consider the rate of the population as well as decay of a particular state with known branching ratios. For the states where a side-feeding component was present, the curves were simulated by assuming an unobserved single state with variable mean life. The decay curves are plotted in Fig. 3 along with the fits (shown by solid lines), for the $2^+ \rightarrow 0^+$ and $4^+ \rightarrow 2^+$ transitions in ^{142}Ba as well as $2^+ \rightarrow 0^+$, $4^+ \rightarrow 2^+$, $6^+ \rightarrow 4^+$, $8^+ \rightarrow 6^+$, $7^- \rightarrow 6^+$, and $9^- \rightarrow 8^+$ transitions in ^{144}Ba. For ^{144}Ba the statistical fitting error of the energy spectra to obtain $N_{\rm PS}$

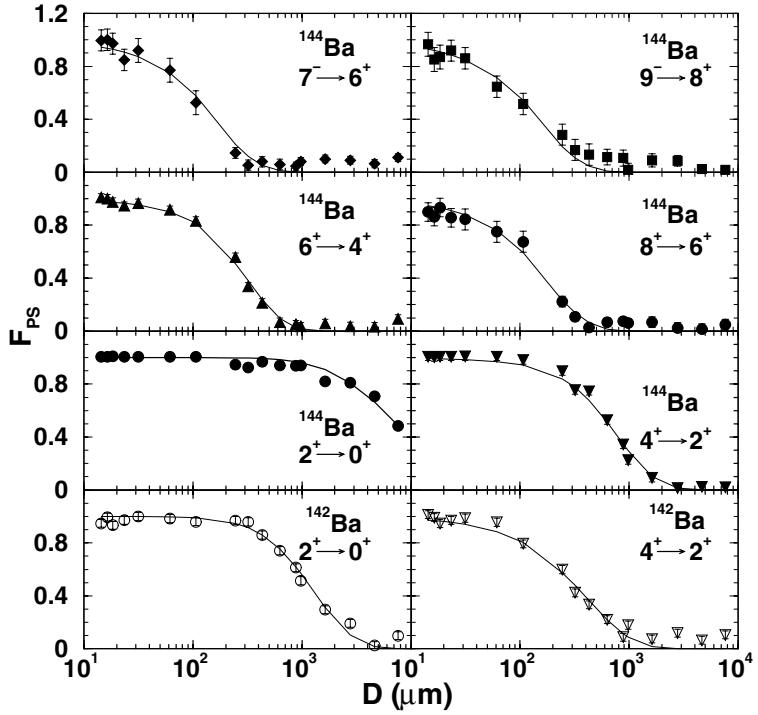

FIG. 3. Decay curves of fractional yields for partial components ($F_{\rm PS}$) as a function of distance between the source and the degrader foil (D) for $E2$ transitions in ^{142,144}Ba and $E1$ transitions in ^{144}Ba. Fits to the data are shown by solid lines.

TABLE I. Lifetimes, τ, and transition quadrupole moments, Q_t, for the yrast bands of ^{142,144}Ba. For comparison previously measured values are also presented.

Nucleus	$I^\pi(\hbar)$	E_γ (keV)	τ^{present} (ps)	τ^{previous} (ps)	Q_t^{present} (e b)	Q_t^{previous} (e b)
^{144}Ba	2^+	199.3	1140 ± 70	1024 ± 40[a]	3.38 ± 0.12	3.29 ± 0.06[a]
	4^+	330.7	71 ± 6	49 ± 7[a]	3.30 ± 0.16	3.80 ± 0.30[a]
	6^+	431.4	21.8 ± 2.1	29 ± 6[c]	2.83 ± 0.16	2.47 ± 0.27[c]
	8^+	509.3	10.3 ± 1.4	—	2.66 ± 0.20	—
	7^-	393.8	2.7 ± 0.9	5.3 ± 1.0[d]	7.3 ± 1.4	5.2 ± 0.6[d]
	9^-	302.3	13.9 ± 4.0	—	2.30 ± 0.37	—
^{142}Ba	2^+	359.6	119 ± 12	93.79 ± 2.9[a]	2.40 ± 0.11	2.67 ± 0.03[a]
	4^+	475.1	24.9 ± 3.7	17.17 ± 1.3[b]	2.18 ± 0.09	2.63 ± 0.10[b]

[a]Ref. [17].
[b]Ref. [18].
[c]Ref. [20].
[d]Ref. [23].

and N_{FS} is about 5% for the excited states in the positive-parity band and about 15% for the 7^- and 9^- states in the negative-parity band. The branching ratio of the feeding states and the uncertainty in the measurement of D are also included in calculating the overall error in determining τ. The lifetime values measured for excited states in ^{142,144}Ba along with the previously measured values for these nuclei are listed in Table I. In the case of ^{142}Ba, the lifetimes were measured only for the 2^+ and 4^+ states. For these states, the values of τ are comparable with the previously measured values, which are obtained from the direct timing of β-delayed γ rays [17]. It can be seen that in the case of ^{144}Ba, the lifetime values decrease sharply from 1140 ps for the 2^+ to less than 100 ps for higher excited states. However, in contrast, a relatively shorter (119 ps) value of τ in ^{142}Ba for the 2^+ state is observed. The lifetimes of the 7^- and 9^- states of the negative-parity band decaying by $E1$ transitions in ^{144}Ba are also measured in the present work. It is observed that the measured lifetime of the 9^- state is large in comparison to the 7^- and the 8^+ states. The branching ratio $B(E1)/B(E2)$ is significantly larger for the 9^- state in comparison to the 7^- state [7], which also suggests the possibility of a longer lifetime for the 9^- state. As the octupole collective 9^- state is long lived, its decay-out component to the 8^+ and 7^- states via $E1$ and $E2$ transitions, will have a strong influence on the measured lifetimes of these states.

D_0 and Q_t are related to τ of any excited state of angular momentum I_i decaying to I_f by a $E1$ or $E2$ transition and obtained from the known reduced transition rates, $B(E1)$ and $B(E2)$ using the rotational model formulae [4]:

$$B(E1) = \frac{3D_0^2}{4\pi}\langle I_i 010|I_f 0\rangle^2 \tag{3}$$

$$B(E2) = \frac{5Q_t^2}{16\pi}\langle I_i 020|I_f 0\rangle^2, \tag{4}$$

where $\langle I_i 010|I_f 0\rangle$ and $\langle I_i 020|I_f 0\rangle$ are the Clebsch-Gordan coefficients.

Although ^{142,144}Ba are not good rotors, the use of these formulae allows a consistent comparison of the experimental results and model calculations. The deduced Q_t for ^{142,144}Ba are listed in Table I, and the D_0 values are given in Table II. For comparison, previously measured values in these nuclei are also presented. It is observed that for the 7^- state, D_0 is large in comparison to the 9^- state, in contrast to the earlier reported values obtained from the branching ratio measurement [4,7]. However, the average value of D_0 for the 7^- and 9^- states is comparable with the theoretical calculations [4,6]. In Fig. 4, the quadrupole moment has been plotted against angular momentum I for the ^{142,144}Ba nuclei. The experimental Q_t values show overall good agreement with the previously measured values for both the nuclei. It is also observed that for ^{144}Ba, Q_t decreases gradually with angular momentum, which is possibly due to a band crossing. The theoretically calculated Q_0 for both the nuclei, is also shown with a dashed line assuming a constant value at higher excited states, and overall

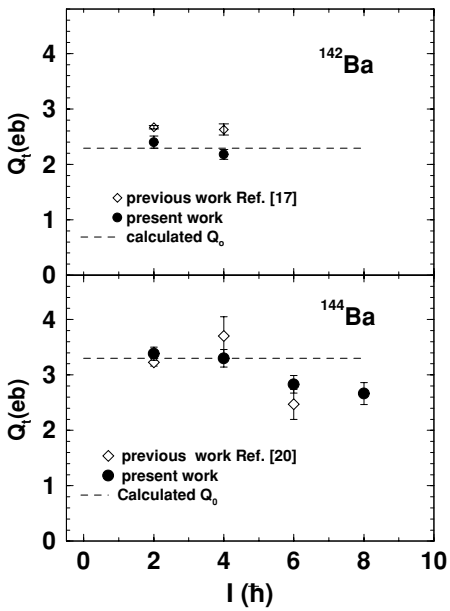

FIG. 4. Transition quadrupole moment, Q_t, in the yrast band of ^{142,144}Ba, plotted against angular momentum, I, of the decaying states. The dashed line represents the ground state quadrupole moment, Q_0 [24].

TABLE II. Lifetimes, τ, and electric dipole moments, D_0, for ^{144}Ba along with the previous values from $B(E1)/B(E2)$ and lifetime measurements. For 7^- and 9^- states, experimental branching ratios are taken to be $\lambda = 0.26$ and 0.84, respectively [7].

I^π ($\hbar$)	τ^{present} (ps)	τ^{previous} (ps)	D_0^{present} (e fm)	D_0^{previous} (e fm)	D_0^{Theory} (e fm)
7^-	2.7 ± 0.9	5.3 ± 1.0[a]	0.17 ± 0.03	0.12 ± 0.01[a]	0.12[c]
				0.07 ± 0.01[b]	0.15[d]
9^-	13.9 ± 4.0	—	0.09 ± 0.01	0.13 ± 0.01[b]	0.12[c]
					0.15[d]

[a]Ref. [23].
[b]Ref. [7].
[c]Theoretical values are taken from Ref. [4].
[d]Theoretical values are taken from Ref. [6].

the experimental data agree with the theoretical predictions of Möller *et al*. [24]. From the lifetime values of the 9^- and 7^- states and known branching ratios, the quadrupole moments are deduced in the negative-parity band. For the $9^- \rightarrow 7^-$ transition, $Q_t = 2.3(4)$ e b and for $7^- \rightarrow 5^-$, $Q_t = 7.3(14)$ e b. It is found that the quadrupole moment for the $9^- \rightarrow 7^-$ transition is similar to that of the positive-parity band. However, it is significantly large for the $7^- \rightarrow 5^-$ transition, which is consistent with the earlier measurement [$Q_t = 5.2(6)$ e b] by Krücken *et al*. [23]. The 7^- state is fed through the 8^+ and 9^- states, having longer lifetime, and it is also possible that other unobserved decay branches may be responsible for the large value of the quadrupole moment for the 7^- state. A large value of the quadrupole moment [$Q_t = 4.6(8)$ e b] has also been observed earlier for the $3^- \rightarrow 1^-$ transition in the negative-parity band in ^{146}Ba [17].

In summary, lifetimes of the excited states in the positive-parity band of ^{142,144}Ba are measured using the differential Doppler shift method. The lifetimes of the 7^- and 9^- states in the negative-parity band are measured in case of ^{144}Ba to obtain directly the electric dipole moment and the quadrupole moments in the negative-parity band. In the negative-parity band in ^{144}Ba, Q_t for the $9^- \rightarrow 7^-$ transition is similar to that of the positive-parity band, but it is surprisingly large for the $7^- \rightarrow 5^-$ transition. For the positive-parity band in both ^{142,144}Ba, the deduced quadrupole moments show good agreement with previous measurements and overall decrease at higher angular momentum in ^{144}Ba. The quadrupole moment of the 7^- level is anomalously large, and further experimental studies as well as detailed theoretical calculations are necessary to understand the properties of the negative-parity octupole band.

We are grateful to W. R. Phillips for useful discussions. The experiment was facilitated by support from the European Union through EUROVIV contract (HPRI-CT-1999-00078). The authors thank the Office of Basic Energy Sciences, U.S. Department of Energy, for supplying the ^{252}Cf source.

[1] G. A. Leander, Nucl. Phys. **A453**, 58 (1986).
[2] W. Nazarewicz, G. A. Leander, and J. Dudek, Nucl. Phys. **A467**, 437 (1987).
[3] S. Åberg, H. Flocard, and W. Nazarewicz, Ann. Rev. Nucl. Part. Sci. **40**, 439 (1990).
[4] P. A. Butler and W. Nazarewicz, Nucl. Phys. **A533**, 249 (1991); Rev. Mod. Phys. **68**, 2 (1996).
[5] W. Nazarewicz and S. L. Tabor, Phys. Rev. C **45**, 2226 (1992).
[6] J. L.Egido and L. M. Robledo, Nucl. Phys. **A545**, 589 (1992).
[7] W. R. Phillips, I. Ahmad, H. Emling, R. Holzmann, R. V. F. Janssens, T. L. Khoo, and M. W. Drigert, Phys. Rev. Lett. **57**, 3257 (1986).
[8] W. R. Phillips, R. V. F. Janssens, I. Ahmad, H. Emling, R. Holzmann, and T. L. Khoo, Phys. Lett. **B212**, 402 (1988).
[9] W. Urban *et al*., Nucl. Phys. **A454**, 213 (1986); Nucl. Phys. **A613**, 107 (1997).
[10] S. J. Zhu *et al*., Phys. Rev. C **60**, 051304 (1999).
[11] A. Lindroth, B. Fogelberg, H. Mach, M. Sanchez-Vega, and J. Bielcik, Phys. Rev. Lett. **82**, 4783 (1999).
[12] J. F. Smith *et al*., Phys. Rev. Lett. **75**, 1050 (1995).
[13] W. Urban *et al*., Eur. Phys. J. A **16**, 303 (2003).
[14] I. Wiedenhover *et al*., Phys. Rev. Lett. **83**, 2143 (1999).
[15] A. G. Smith *et al*., Phys. Rev. Lett. **73**, 2540 (1994).
[16] A. G. Smith *et al*., Phys. Rev. Lett. **77**, 1711 (1996).
[17] H. Mach, W. Nazarewicz, D. Kusnezov, M. Moszynski, B. Fogelberg, M. Helstrom, L. Spanier, R. L. Gill, R. F. Casten, and A. Wolf, Phys. Rev. C **41**, R2469 (1990).
[18] G. Mamane, E. Cheifetz, E. Dafni, and A. Zemel, Nucl. Phys. **A454**, 213 (1986).
[19] A. G. Smith *et al*., J. Phys. G **28**, 2307 (2002).
[20] R. Krücken *et al*., Phys. Rev. C **64**, 017305 (2001).
[21] R. Krücken *et al*., Phys. Rev. Lett. **88**, 232501 (2002).
[22] C. Hutter *et al*., Phys. Rev. C **67**, 054315 (2003).
[23] R. Krücken *et al*., Eleventh International Symposium on Capture Gamma-Ray Spectroscopy and Related Topics-CGS11, Prague, Czech Republic, Sept. 2002, edited by J. Kvasil, P. Cejnar, and M. Krticka, (World Scientific), p128.
[24] P. Moller, J. R. Nix, W. D. Myers, and W. J. Swiatecki, At. Data Nucl. Data Tables **59**, 185 (1995).